Fusion Engineering and Design 201 (2024) 114229

Contents lists available at ScienceDirect

Fusion Engineering and Design

journal homepage: www.elsevier.com/locate/fusengdes

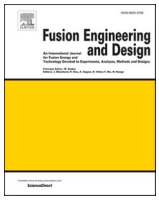

Thermal and structural analysis of TCABR vacuum vessel during baking process

Pedro Leo Oliveira Marques [a,*], Ruy Marcelo de Oliveira Pauletti [a], Juan Iraburu Elizondo [b]

[a] Polytechnic School of the University of São Paulo, São Paulo, Brazil
[b] Physics Institute of the University of São Paulo, São Paulo, Brazil

ARTICLE INFO

Keywords:
Tokamak
Vacuum vessel
Baking
Thermal stress

ABSTRACT

TCABR is a small-sized tokamak located at the University of São Paulo, in Brazil. It is planned to undergo an extensive upgrade, which includes a baking system. However, this tokamak wasn't designed considering baking as a possible wall conditioning technique. This paper analyzes whether a baking system with ohmic heating could in principle be installed on TCABR, considering the thermal stresses that it might produce on the vacuum vessel. An analytical steady-state heat transfer model was used to estimate the heat fluxes required to reach a target temperature of 200 °C. Thermal and structural transient finite element method models were developed using ANSYS Workbench®. The temperature distribution was used to calculate the thermal stresses, also considering the effects of gravity and vacuum pressure. The stresses produced in the vacuum vessel by baking were below the limit defined by the ASME stress code, but the graphite tiles' support rails reached stress values above their material's yield strength. The resulting temperature distribution was not uniform, with some regions far from the 200 °C target. A redesign of the baking system will be required to reach a more uniform temperature field and avoid stresses above yield strength for some components.

1. Introduction

TCABR (Tokamak à Chauffage Alfvén Brésilien) is a small-sized tokamak located at the Physics Institute of the University of São Paulo, in Brazil, and is shown in Fig. 1. It has a major radius $R_0 = 0.62\ m$ and plasma minor radius $a \leq 0.2\ m$. Originally conceived as the TCA tokamak, it was acquired from the École Polytechnique Fédérale de Lausanne (EPFL) and transported to Brazil, where it received the suffix "BR" and began operating in 1999 [1]. The TCABR is currently undergoing an extensive upgrade, which includes the installation of graphite tiles to form a first wall, completely covering the vacuum vessel's inner wall [2], and a baking system, which has the goal of removing impurities from the graphite tiles and vacuum vessel inner walls, improving the conditions inside the vessel to produce plasma. The baking system is currently at the design phase, and the initial concept consists of installing ohmic heating elements on the vessel outer walls and covering the vessel and heating elements with a thermally insulating blanket. The objective is to indirectly heat the graphite tiles to 200 °C by heating the vacuum vessel and allowing the heat to reach the graphite tiles through conduction and thermal radiation. However, TCABR wasn't designed considering baking as a possible wall conditioning technique. Heating the vacuum vessel will cause thermal expansion, which produces stresses on the vessel and structural components attached to it. The thermal stresses produced by the installation of this baking system can cause significant damage to the vessel structure, and therefore must be properly analyzed.

Several studies have been conducted on the effects of baking on the vacuum vessels of different tokamaks, such as SST-1 [3], EAST [4], KSTAR [5], DIII-D [6], TPX [7], KTM [8], T-15MD [9] and HL-2M [10]. The literature provides some insights into the successful design of a baking system. Firstly, tokamaks with a double wall configuration, like EAST and KSTAR, manage to achieve low temperature gradients, which contribute to reduce the thermal stresses, by using hot pressurized gas flowing between the inner and outer walls. Secondly, tokamaks that use ohmic heating have been shown to achieve a large temperature gradient, such as T-15MD. This is undesirable not only due to the thermal stresses, but also because it reduces the effectiveness of impurity removal. Thirdly, the process must be analyzed in the transient state, since the largest values of thermal stress may happen well before arriving at the steady state [7,11]. Lastly, vacuum vessels with a rigid support system may achieve stress values above the allowable design limits, while

* Corresponding author.
E-mail address: pedro.leo.marques@usp.br (P.L.O. Marques).

https://doi.org/10.1016/j.fusengdes.2024.114229
Received 13 November 2023; Received in revised form 10 January 2024; Accepted 5 February 2024
Available online 22 February 2024

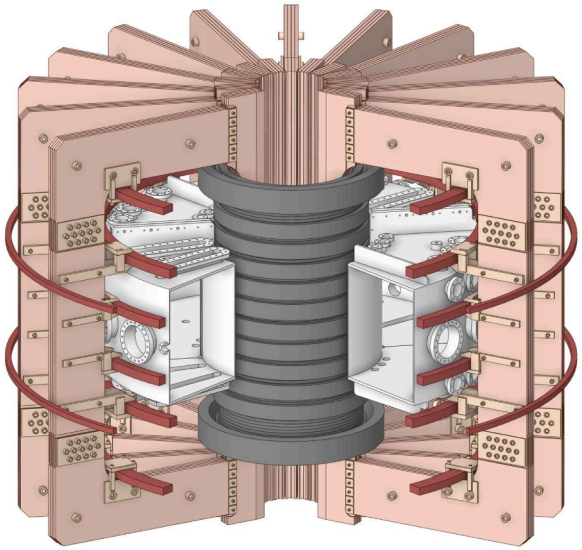

Fig. 1. 3D model of TCABR tokamak.

vessels with more flexible supports that allow movements in the radial direction, such as EAST, KSTAR and HL-2M, manage to achieve stress values low enough for the stress criteria to be satisfied.

Given these considerations, the present paper aims to study the viability of the proposed baking system for the TCABR tokamak. TCABR doesn't have a double-wall configuration, its vacuum vessel has a rigid support structure, and the proposed baking system uses ohmic heating. Therefore, the objective is to check whether this type of baking system would be capable of raising the temperature of the graphite tiles to 200 °C while keeping the thermal stresses in the vacuum vessel below the limits calculated by the relevant stress criteria. If the stresses are above the limits, the authors will analyze what changes must be made to the baking system and possibly to other components, such as the support columns, to reduce the stresses to acceptable values. The conclusions in this paper will serve as a direction for future studies.

2. Materials and methods

In order to analyze the thermal and structural effects of baking on TCABR vacuum vessel, an initial design for the baking system was conceived and the relevant components for the analysis were defined. Their materials were also defined, so that the relevant thermal and structural properties could be eventually used. A geometrical model was built for the finite element method simulations. An analytical one-dimensional heat transfer model was developed to estimate the heat fluxes that would have to be supplied by the baking system to heat the graphite tiles to the target temperature of 200 °C. These values were adapted to the 3D model and used on the tridimensional transient-state heat transfer model, developed on ANSYS Workbench® [12], along with the relevant boundary and initial conditions. The resulting time-dependent temperature distribution was then used as input for the transient structural model. After solving both the thermal and structural FEM models, the resulting equivalent stresses were compared to the limit calculated by the elastic ratcheting analysis method, present in the "Design by Analysis Requirements" part of the ASME Boiler and Pressure Vessel code, Section VIII, Division 2 [13], to protect the vessel against failure from cyclic loads. This comparison was performed to determine if the proposed baking system would be structurally safe, and therefore a viable option for TCABR, or if changes would have to be made to the baking system or any other components to satisfy the stress criteria. The following subsections provide the details of the aforementioned procedure.

2.1. TCABR vacuum vessel structure and materials

TCABR is a small-sized tokamak. Its vacuum vessel is made of 316L stainless steel and has a rectangular cross section with 445 *mm* width and 520 *mm* height. The radius of the external inboard wall is 395 *mm*, while the radius of the external outboard wall is 850 *mm*. The vertical walls of the vessel are 5 *mm* thick, while the horizontal walls are 12 *mm* thick. There are several ports all around the vessel, with different sizes and functions. They are distributed in a non-symmetrical way. The vessel is comprised of two halves, which are connected by flanges, welded on each side of the vessel. Between the flanges there is currently a Viton elastomer gasket, which is placed around a 316L stainless steel rectangular frame, to keep the gasket in shape and at the correct position. This material will be substituted during the upgrade. A few options are being considered, such as using Kalrez instead of Viton, or copper gaskets along with ConFlat-type channels, which would have to be machined onto the flanges. This would make the vessel electrically conductive in the toroidal direction, which is beneficial for plasma position stability. Fig. 2 shows the vacuum vessel during the first assembly of TCA tokamak at EPFL.

Each side of the vessel has two tubular support lugs with reinforcing ribs welded to the vessel's bottom walls. A cylindrical steel component is partially inserted into each support lug. This component is also partially inserted into a support column, 1.665 *m* in height, with external diameter of 100 *mm* and internal diameter of 80 *mm*. The bottom of each column is welded to a large stainless-steel base plate, which is fixed to a concrete foundation below the tokamak. The cylindrical connecting component rests inside the support column, allowing the vessel to be supported by them. These connecting components are also covered by PVC tubes, to electrically isolate the vessel from the support columns. Therefore, there are in total four steel columns supporting the TCABR vacuum vessel. Fig. 3 illustrates the connection between vacuum vessel and support columns, and the components involved.

The proposed baking system would add ohmic heating elements to the outside walls of the vessel. They are currently at the design phase, and therefore were not included as geometrical components in the simulations. They were instead represented by heating areas placed on the vacuum vessel outer walls. However, their current design consists of Ni-Cr alloy wires, insulated with ZnO_2 powder and housed inside copper tubes, which would be installed inside channels machined onto the bottom of aluminum plates. These plates would be fixed to the vessel by

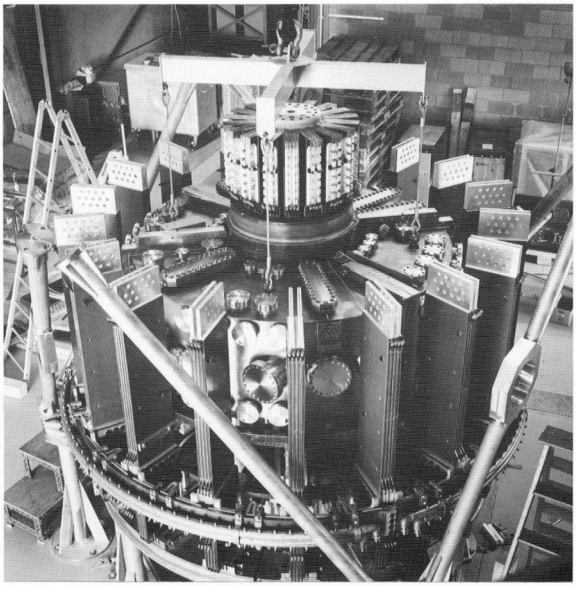

Fig. 2. TCA first assembly at EPFL [14]. Vacuum vessel in center, around central solenoid.

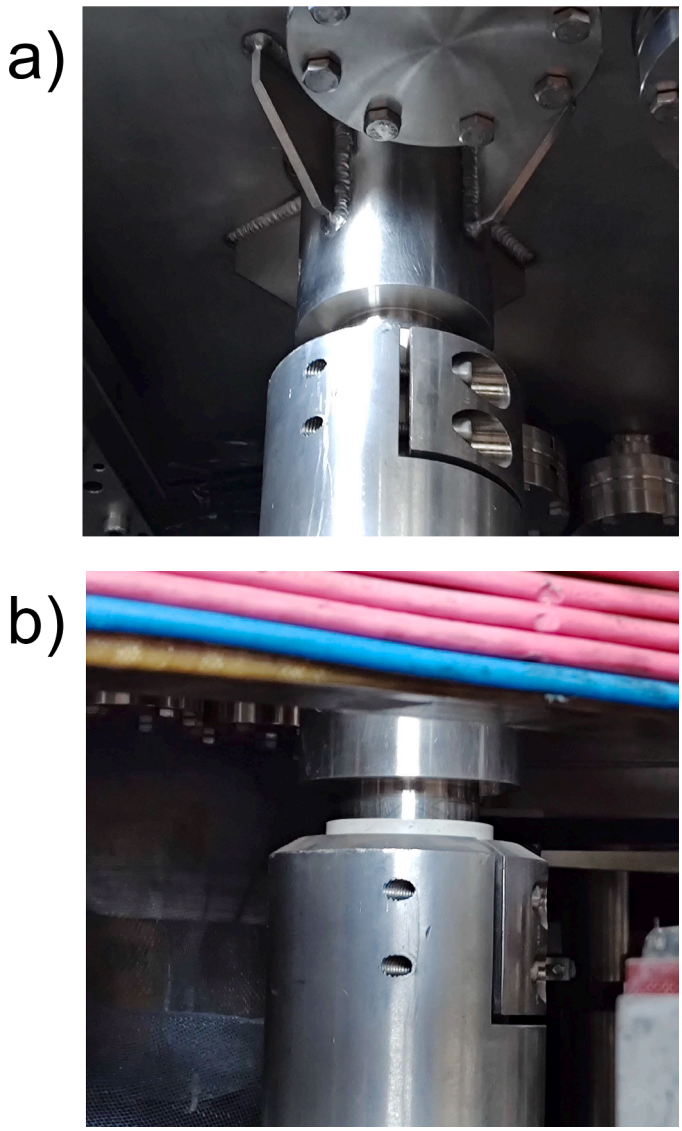

Fig. 3. (a) Support lug. (b) Connection between vacuum vessel and support column. PVC tube in white.

screwing them into nuts, which would be welded to the vessel outer walls beforehand. Between the plates and the vessel a thermal paste would be applied, to provide the necessary thermal contact between the components. Fig. 4 shows a 3D version of the preliminary heating element design.

As part of the baking system, an Alumina fiber blanket, 6.5 mm thick, would be used to cover the vacuum vessel, ohmic heating elements, and the vessel support columns, to reduce the amount of heat lost to the environment. This thickness has been currently chosen due to constraints on the space available around the vessel, particularly at the inboard region. It was assumed in this study that the Alumina blanket was entirely in contact with the components, with no gaps between them.

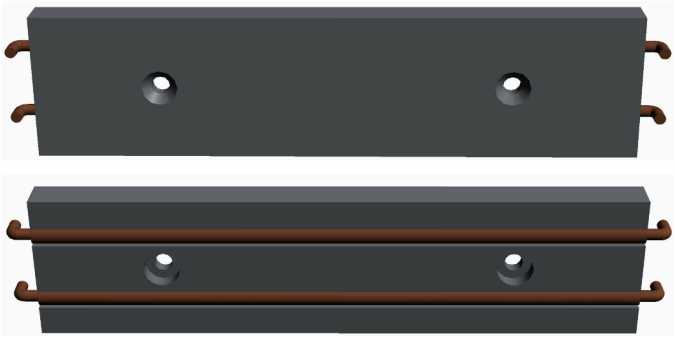

Fig. 4. Current heating element conceptual design.

The TCABR tokamak upgrade also includes the installation of graphite tiles inside the vessel, to form a new first wall for the plasma. These tiles would be supported by 316L stainless steel support rails welded inside the vessel. The baking system would also require the PVC tube to be substituted by another electrically isolating tube but made of a material capable of withstanding temperatures up to 200 $^{\circ}C$, such as silicone or KTM rubber. Fig. 5 illustrates the 3D model of the vacuum vessel and the components used in the simulations (except for the ohmic heating elements, as previously discussed) while Table 1 lists the materials present in the whole model and some of their thermal properties.

2.2. Analytical heat transfer model

In order to estimate the heat fluxes required to heat the graphite tiles to the target temperature of 200 °C, a simple analytical, one-dimensional, steady-state heat transfer model was developed. Steady state was chosen for this model because the baking system goal is to maintain the graphite tiles at the target temperature of 200 °C for several hours, representing, therefore, a steady state condition for the system.

On the outside of the vacuum vessel, the heat transfer mechanisms considered in the model were natural convection and radiation from the Alumina fiber blanket to the environment. Inside the vessel only thermal radiation exchange was considered, but occurring on two types of regions: between the vacuum vessel internal walls and the graphite tiles, and only between the graphite tiles through the region enclosed by them. One also expects conduction to occur on each component and across the interfaces between components, e.g. from vessel to Alumina blanket. Fig. 6 illustrates the one-dimensional model developed.

During steady state, one can assume that both internal and external faces of the graphite tiles have reached 200 °C. Modelling the graphite tiles and vacuum vessel as two parallel walls with gray, diffuse surfaces, the equation that describes the heat transfer is given by [15]:

$$\dot{Q}_{1,2} = A\sigma\left(T_g^4 - T_w^4\right) \Big/ \left(1/\epsilon_g + 1/\epsilon_w - 1\right) \tag{1}$$

In Eq. (1), A is the heat transfer area, σ is the Stefan-Boltzmann constant, T_g and ϵ_g are the graphite tile outer face temperature and emissivity, and T_w and ϵ_w are the vacuum vessel internal wall temperature and emissivity. During steady state the net heat flux between the surfaces, as in Eq. (1), must be zero. Therefore, one can conclude that the temperature of the internal vacuum vessel walls must also be equal to 200 °C to satisfy this condition. This leads to $T_w = 200\ ^{\circ}C$. Using this temperature as a boundary condition for the vacuum vessel's internal wall in this one-dimensional model and including as boundary conditions the loss of heat from the Alumina fiber blanket to the environment by natural convection and radiation, one obtains the following equation for the heat flux:

$$q = k_w\frac{(T_w - T_i)}{L_w} = k_b\frac{(T_i - T_b)}{L_b} = h(T_b - T_{env}) + \sigma\epsilon_b\left(T_b^4 - T_{env}^4\right) \tag{2}$$

Rearranging the equation in terms of the Alumina blanket external wall temperature, it becomes:

$$r_{eq}\sigma\epsilon_b T_b^4 + \left(r_{eq}h + 1\right)T_b - \left[r_{eq}\left(\sigma\epsilon_b T_{env}^4 + hT_{env}\right) + T_w\right] = 0 \tag{3}$$

Where $r_{eq} = (L_w/k_w + L_b/k_b)$. Therefore, knowing the parameters L_w, k_w, L_b, k_b, ϵ_b, h, T_{env} and T_w (which has been determined to be 200 $^{\circ}C$ by the previous discussion), this equation can be solved for the Alumina blanket temperature T_b, and using Eq. (2) one can obtain the

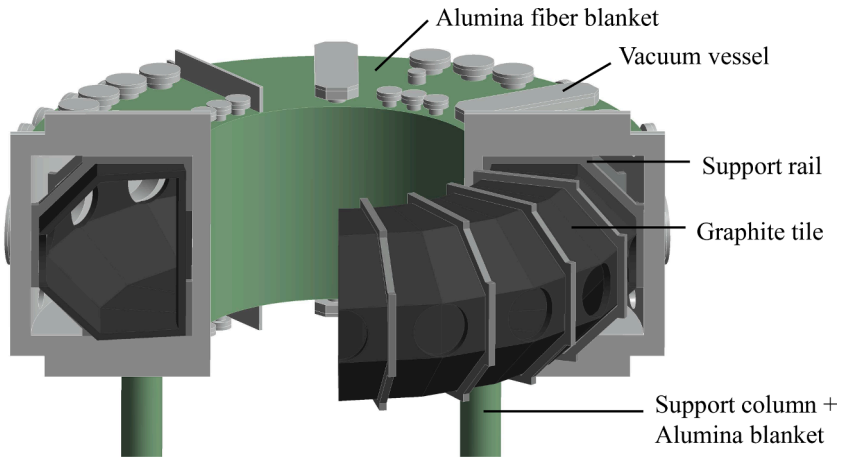

Fig. 5. Cut view of components modeled for the simulations.

Table 1
List of materials present in the system and their thermal properties.

Material	Thermal conductivity (W/mK)	Specific heat $(J/kg\,K)$	Density (kg/m^3)	Total Normal emissivity
316L stainless steel	15	500	8000	0.1
Alumina fiber blanket	0.06	1000	100	0.9
Graphite	70	750	1760	0.7
KTM rubber	0.18	974	1900	–

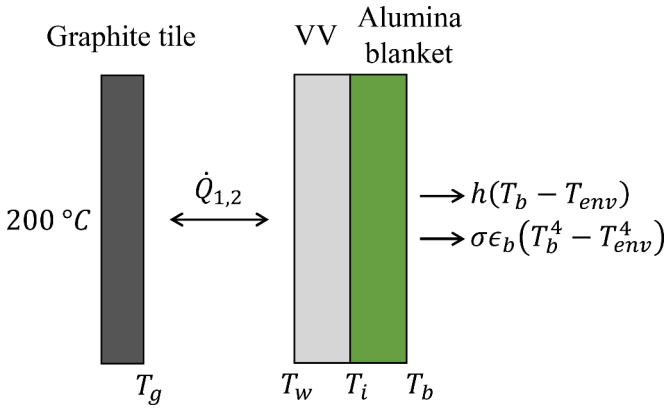

Fig. 6. One-dimensional heat transfer model used to estimate baking heat fluxes.

heat flux required to reach such condition.

Out of these parameters, the natural convection heat transfer coefficient h is the only one not clearly defined, since it is a function of the Alumina blanket temperature T_b. Its value has been calculated for each type of vessel wall (top, outboard, bottom, inboard) by choosing the correlations between Nusselt and Rayleigh numbers that most closely approximate the wall geometries and heat transfer situations. The correlations were extracted from Çengel [15], Bejan [16] and Rohsenow et al. [17]. An iterative method was used to find the steady-state values of h and T_b for each wall. After defining these values, the heat flux required to keep the system in steady state was calculated using Eq. (2). Table 2 lists the types of *Nu* correlations used for each external surface, and the resulting values of heat transfer coefficients and heat fluxes on each type of wall.

Table 2
Correlations used for each type of external wall and values of steady state h and q obtained.

External wall	Correlation	Steady state h (W/m^2K)	Steady state heat flux q_{sur} (W/m^2)
Top	Hot upwards horizontal plate	6.85	1001
Outboard	Vertical plate	5.72	975
Bottom	Hot downwards horizontal plate	2.97	890
Inboard	Parallel Isothermal Plates	4.41	937

2.3. Finite element heat transfer model

During the baking process, the vacuum vessel external walls will receive the heat from the ohmic heating elements. One possible heating scenario has been studied. This scenario applies the heat fluxes on specific regions on each vessel wall, where the ohmic heating elements could be installed. Fig. 7 shows in blue the regions where heat fluxes were applied on the TCABR vacuum vessel, in the finite element heat transfer simulation.

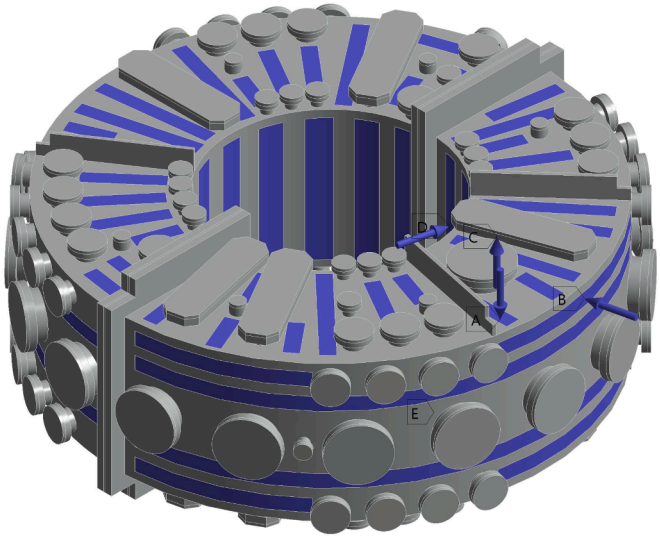

Fig. 7. Heating areas (in blue) representing the ohmic heating elements. (For interpretation of the references to color in this figure legend, the reader is referred to the web version of this article.)

It was implicit in the one-dimensional analytical model that the heat fluxes and temperatures were evenly distributed. That is, variations of physical quantities only occur in the horizontal direction of the model in Fig. 6. The values of heat fluxes shown on Table 2 were obtained for this one-dimensional model. However, this is not the case for the finite element heat transfer model developed. Given that the finite element model is tridimensional, and the heating is applied unevenly, at specific areas around the vessel, new values must be calculated to compensate for these facts. The actual values used in the simulation, defined as q_{elem}, were obtained by multiplying the heat fluxes in Table 2 by the ratio between the area of the wall and the area covered by the ohmic heating elements installed on that type of wall. The values of q_{elem} were then applied to each heating element area, according to the type of wall where they were located. Table 3 shows the values of heat fluxes q_{elem} used on the thermal model, on each type of VV external wall. The total heating power supplied to the system, calculated using q_{elem} and the covered areas in Table 3, is 6336 W.

Given that this model was developed in transient state, the time dependence of the heat fluxes must be defined. Instead of limiting the temperature ramp-up to a specific value per hour (°C/hr), the heat fluxes in Table 3 were applied to the system in a two-step method, divided into the first 12 hours and the remaining 13 hours of simulation. During the first 12 hours the heating was supplied using ramp functions. The heat fluxes at each heating area increased from zero, at the beginning of the simulation, to the values shown in Table 3 at the 12-hour mark, according to the wall where they are located. After this instant they were kept constant for the remainder of the simulation. The numerical results show that the maximum temperature increase during the simulation using this heating method was 11.6 °C/hr.

The values of natural convection heat transfer coefficient h for each type of correlation were introduced in this model as tabular data, mapping the Alumina blanket external temperature to the value of h calculated by the appropriate correlation. Fig. 8 illustrates how the values of h vary for each type of wall.

2.4. Structural model

The structural model considers three types of loadings: The dead weight (D) of all the components in the model; the pressure difference (P) of 1 *atm* between the inside and outside of the vacuum vessel, and the thermal stresses (T) produced by the temperature field resulting from the thermal model. Therefore, there is a one-way coupling between models, from the thermal to the structural one. Table 4 lists the mechanical properties of the 316L stainless steel. The structural analysis of the graphite tiles has been left for future works, since the objective of this paper is to analyze the effects of baking on the TCABR vacuum vessel. The Alumina fiber blanket wasn't included in the structural model, given its low density and resistance. The structural model included only the vacuum vessel, graphite tiles support rails, and the support structure components.

2.5. ASME stress code

The stress code used to analyze the viability of the proposed baking system is the ASME Boiler and Pressure Vessel code, Section VIII, Division 2, more specifically the design by analysis methodology. Given the cyclic nature of the baking process and the mechanical and thermal loads considered in the analysis, the code recommends using the elastic ratcheting analysis method, comparing the primary and secondary stresses $(P_L + P_b + Q)$ to three times the average of the allowable stress S in the operating temperature range, to protect the vessel against failure from cyclic loads. Since this criterion requires primary and secondary stresses to be analyzed together, stress linearization was not used. The values of allowable stress have been obtained from ASME BPVC, Section II, Part D (2010) [18], for the temperatures of 20 °C and 200 °C. The resulting average allowable stress is 112 *MPa*. Therefore, the stresses $(P_L + P_b + Q)$ must be compared to 336 *MPa*.

Table 3
Heat flux values applied on heating areas of each type of wall.

External VV wall	Total Area (m^2)	Covered Area (m^2)	Ratio	Heat flux q_{elem} (W/m^2)
Top	1.51	0.45	3.4	3359
Outboard	2.34	0.74	3.2	3083
Bottom	1.50	0.45	3.3	2967
Inboard	1.29	0.61	2.1	1981

2.6. Coupled finite element method model

The thermal and structural finite element method models previously discussed were developed using three-dimensional continuum elements and were solved in the transient state. A one-way coupling was defined, from the thermal model to the structural one, to allow the time-dependent temperature distribution to be used as input in the structural analysis.

The thermal model used the quadratic tetrahedral, hexahedral and wedge elements Tet10, Hex20 and Wed15, respectively. The resultant finite element model had 535,243 nodes and 211,973 elements. A simulation time of 25 h (90,000 s) was defined, with a sub-step time of 10 min. The heat fluxes were applied on the external vacuum vessel walls in the two-step method mentioned in subsection 2.3. The initial condition was that all components were at the ambient temperature of 20 °C. The boundary conditions were heat loss by natural convection from the Alumina blanket external walls, using the tabular data for each coefficient as a function of surface temperature; heat loss by radiation from the blanket external walls to the environment; radiation heat transfer between vacuum vessel inner walls and graphite tiles; and radiation heat transfer between the graphite tiles inner faces. The emissivity values used for the radiation conditions are shown in Table 1.

The structural model also used the quadratic tetrahedral, hexahedral and wedge elements Tet10, Hex20 and Wed15, resulting in 658,305 nodes and 246,228 elements. This model also used a total simulation time of 25 h with a sub-step time of 10 min. All contact regions were defined as bonded, and the bases of all four support columns were determined to be fixed, restraining their movement. The mechanical loadings were the dead weight of all components, a pressure of 1 atm applied to the external faces of the whole vacuum vessel, including ports and their closures, and the temperature field obtained from the thermal model for the components present in this model (vacuum vessel, graphite tiles support rails and vacuum vessel support structures) at each simulation sub-step.

3. Results and discussion

In this heating scenario, there is a considerable difference between the maximum and minimum values of temperature found for the vacuum vessel, going from 114 °C to 239 °C. The maximum values occur at the outboard walls, while the minimum values occur not only at the support lugs where the columns are connected, but also at regions between vertical and horizontal ports where no heat flux has been applied, because it wouldn't be possible to install ohmic heating elements on such locations. Until this moment, the authors were unable to reduce the maximum temperature to 200 °C without also decreasing the minimum temperature on the vessel. The temperature on the graphite tiles ranged from 165 °C to 197.5 °C. Figs. 9 and 10 illustrate the temperature distributions on the vacuum vessel and the graphite tiles after 25 h of baking. Fig. 11 illustrates the temperature change in these components during the simulation.

The maximum stress obtained on the vessel was 250 MPa, at the connection between the vessel and one of the circular ports welded to the outboard wall, near the connecting flanges, as shown in Fig. 12. This

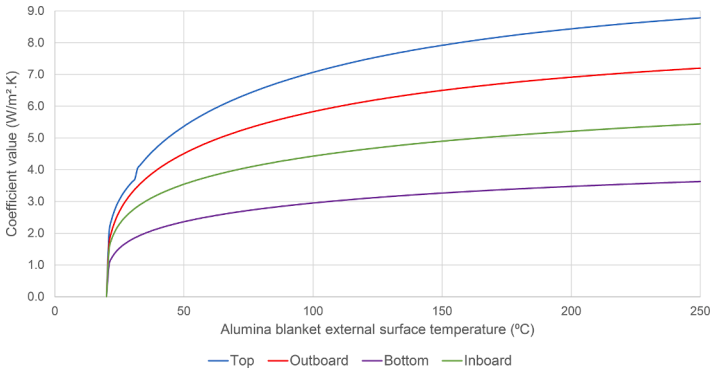

Fig. 8. Values of h for each type of wall as a function of external temperature.

Table 4
Properties and limit stress values of 316L stainless steel.

Material	316L stainless steel
Yield Strength (MPa)	170
Tensile Strength (MPa)	485
Young Modulus (GPa)	193
Thermal Expansion Coefficient (10^{-6} K^{-1})	16.5
Allowable Stress S_m at 20 °C (MPa)	115
Allowable Stress S_m at 200 °C (MPa)	109
Average allowable Stress S (MPa)	112
ASME BPVC calculated limit (MPa)	336

value is below the limit of 336 MPa defined by the stress code for this situation. During the 25 h of baking the maximum stress on the vessel slowly rose to this value. However, the stress acting on the graphite tiles support rails peaked at 289 MPa after 12 h of baking, at a corner connecting one of the rails to the vacuum vessel, and then slowly descended to 223 MPa in 25 h. These values, although below the ASME criteria for ratcheting, are above the yield strength of 316L stainless steel. Considering that the support rails reached an average temperature of 161 °C, the yield strength calculated for this temperature using ASME BPVC Div. II Part D would be 128 MPa. In this case, more support rails reach stress values above this limit, at regions of stress concentration. Fig. 13 shows these problematic regions, while Fig. 14 shows the evolution of maximum stresses during the baking process.

Given these results, it is possible to obtain some insights regarding the baking of the TCABR vacuum vessel. Firstly, the way the heating was applied to the vessel, in terms of spatial distribution and time variation, was unable to produce a satisfactory result for the temperature distribution across the system. The graphite tiles temperatures were sufficiently close to the 200 °C target, but the vessel greatly exceeded such limit. This must be avoided, because such high temperatures could damage some devices that will be installed inside the vessel. Therefore, a new study of the heating system would be required, to find a way of spreading the heat more uniformly across the vessel while staying below the 200 °C limit.

Secondly, the graphite tiles support rails managed to reach maximum stress values above those obtained in the vacuum vessel. Although the maximum values were below the limit calculated by the ratcheting criterion in the ASME BPVC, the support rails used in these simulations are not structures commonly found in pressure vessels, therefore the calculated limit should not be applied to such structures. Limiting the stress on the rails to values below the yield strength of 316L stainless steel would be a more conservative, and possibly safer, approach to the problem. One solution would be to cut the rails around the regions of stress concentration and remove such regions. This would also remove the structural connection provided by the support rail between the vessels vertical and horizontal walls, possibly reducing the stresses on them. More studies would be required to find the best solution.

Lastly, contrary to what the literature review suggested, the rigid support columns used on TCABR weren't a great limiting factor for the baking system, since the maximum stress value obtained for the support columns was 50 MPa, well within the limit defined by the ASME stress code and below 316L stainless steel yield strength. This means for the TCABR a reduction in the upgrade costs, since the vacuum vessel

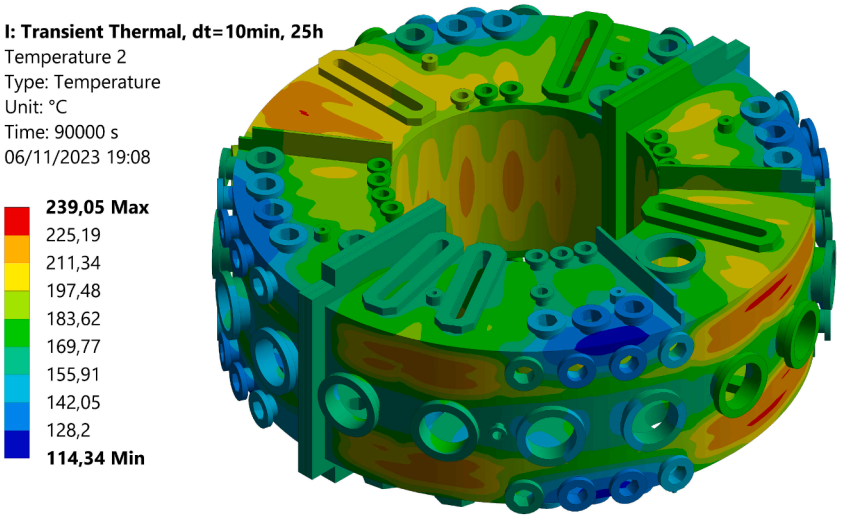

Fig. 9. Vacuum vessel temperature distribution after 25 h of baking.

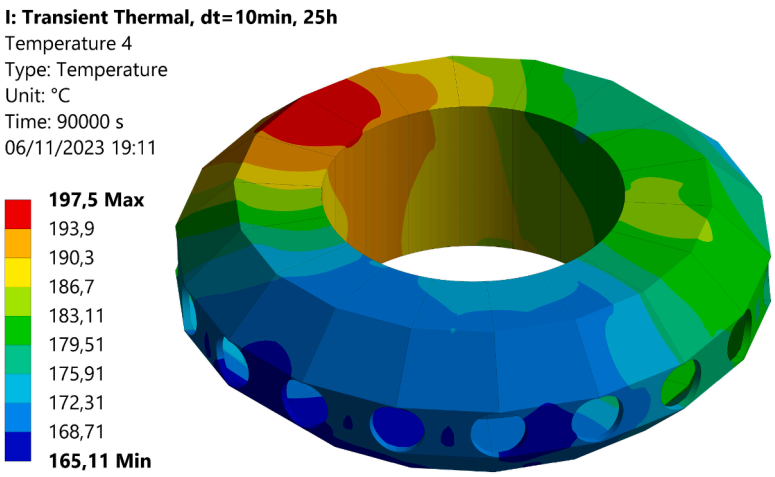

Fig. 10. Graphite tiles temperature distribution after 25 h of baking.

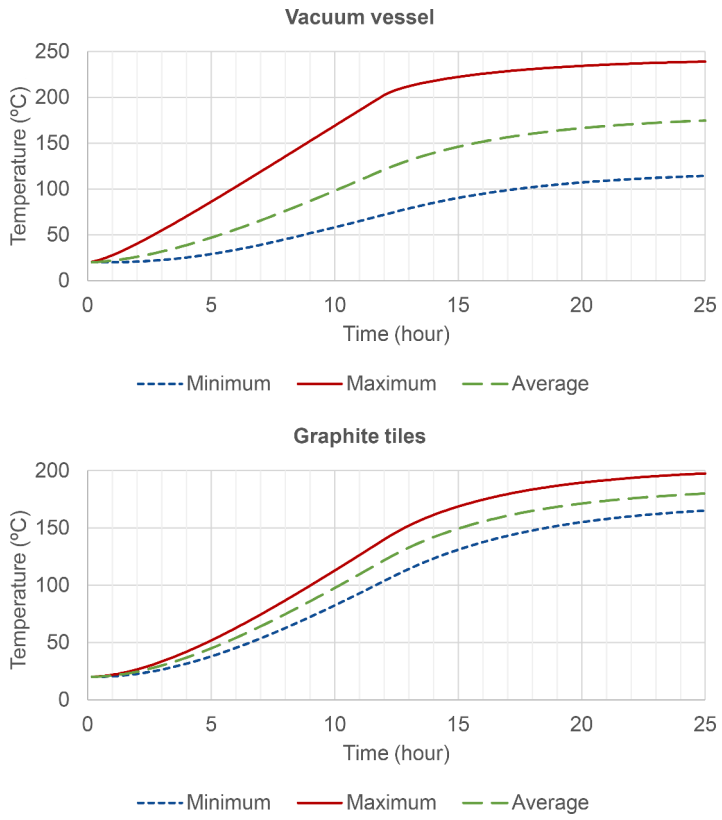

Fig. 11. Temperature evolution in vacuum vessel and graphite tiles during simulation.

supports won't necessarily have to be adapted to reduce their rigidity in the radial direction. This result could also be valuable to other research groups with small-sized tokamaks around the world that wish to install baking systems on their devices. If their tokamaks have rigid support structures, the results indicate that spreading the heating sources as evenly as possible around the vacuum vessel and gradually applying the heat fluxes would be more important than the vacuum vessel support system, giving them the possibility of baking their tokamaks while reducing the associated costs.

4. Conclusions and future works

Thermal and structural analyses using the finite element method software ANSYS Workbench® were performed to assess the theoretical viability of installing a baking system on the TCABR tokamak vacuum vessel, using only ohmic heating. The results indicate that, despite the limitations suggested by the literature review, such as the TCABR vacuum vessel rigid support structure, a baking system using ohmic heating could be, in principle, a viable option for TCABR, from a structural point of view. Despite the large temperature gradients produced by the proposed baking system, the maximum equivalent stresses acting on the vacuum vessel were below the limit calculated by the ratcheting criterion in the ASME Boiler and Pressure Vessel Code. The stresses on the support columns were below both this limit and their material yield strength. However, some graphite tiles support rails reached stress values above their material yield strength at stress concentration

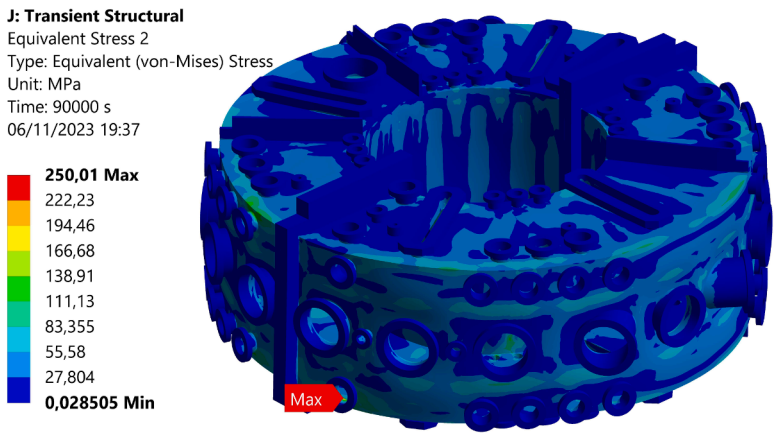

Fig. 12. Equivalent (Von Mises) stresses on vacuum vessel after 25 h of baking.

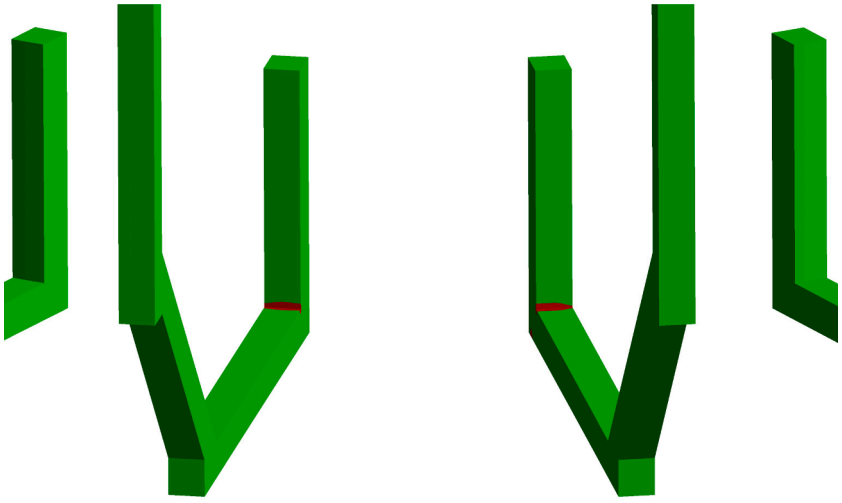

Fig. 13. Regions of equivalent stress at support rails above yield strength, in red, after 25 h of baking.

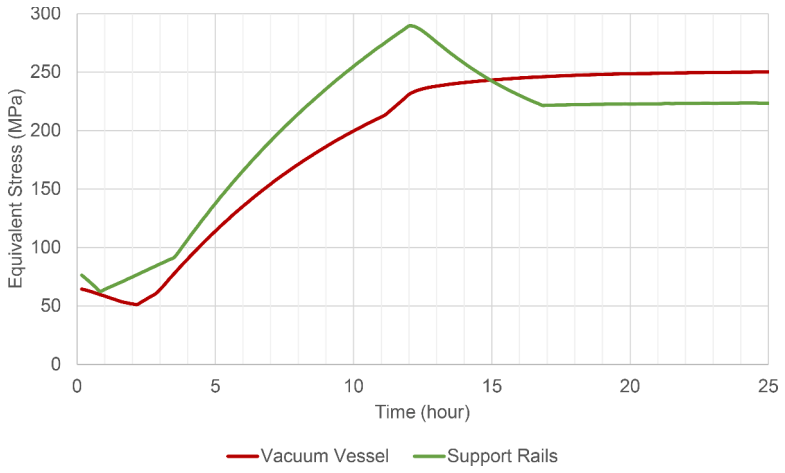

Fig. 14. Evolution of maximum stress on vacuum vessel and support rails during simulation.

regions, indicating the need for a redesign of these components. The proposed baking system produced temperature values above the target temperature of 200 °C, which could cause damage to other components that may be installed inside the vessel as part of the overall upgrade. The large temperature gradient also reduces the baking effectiveness. New estimates for the heat fluxes must be made to avoid this situation. Lastly, the present analysis was based on certain assumptions and simplifications that must be compared against experimental results, to verify their validity. Therefore, more studies must be performed to reach a final design for the TCABR baking system. These future works would be divided into two broad areas: numerical and experimental.

The numerical studies will increase the system's complexity, and

their objective is to improve the model's accuracy. They will analyze how to spread the heat more evenly across the vessel while still using ohmic heating elements, and if using a PID controller to limit the ramp-up temperature to no more than 5 $^{\circ}C/hr$, as previously done in other tokamaks, would limit the stress values obtained even further. The support rails will be redesigned to remove the stress concentration regions. The natural convection heat transfer coefficients estimated in this study will be compared to values obtained from CFD (Computational Fluid Dynamics) models. Lastly, new components that were omitted from this study due to still being at their design phase will be included. These components include equipment that will be attached to the vacuum vessel's ports, thereby imposing new restrictions to the vessel's thermal expansion. A more flexible support system, or one that allows movement in the radial direction, might be necessary in this case and shall be studied. Overall, a more comprehensive structural analysis will be performed to reach a structurally safe design for the baking system.

The experimental studies involve using a small vacuum vessel located at the laboratory, that represents 1/6th of the TCABR vacuum vessel, to test several aspects of the baking system design. These aspects include the heating elements design, the Alumina blanket thickness and material, the installation methods of these components, and the ramp-up control system. The experimental tests will also be used to validate numerical results, such as the natural convection heat transfer coefficients, the resulting temperature distributions, the effects of attaching equipment to the vessel ports, and possible solutions to this matter, such as using bellows or adding heating strips to reduce the temperature gradients in these ports.

These numerical and experimental studies will help arrive at a feasible and effective baking system for TCABR and shall be presented in subsequent works.

CRediT authorship contribution statement

Pedro Leo Oliveira Marques: Conceptualization, Formal analysis, Investigation, Methodology, Writing – original draft, Writing – review & editing. **Ruy Marcelo de Oliveira Pauletti:** Formal analysis, Investigation, Project administration, Supervision, Writing – review & editing, Resources, Writing – original draft. **Juan Iraburu Elizondo:** Formal analysis, Investigation, Methodology, Validation, Writing – original draft, Writing – review & editing.

Declaration of competing interest

The authors declare that they have no known competing financial interests or personal relationships that could have appeared to influence the work reported in this paper.

Data availability

No data was used for the research described in the article.

Acknowledgements

This work was supported by the Coordenação de Aperfeiçoamento de Pessoal de Nível Superior – Brasil (CAPES) – Finance Code 001; and by the São Paulo Research Foundation (FAPESP) [grant #2022/04857-2].

References

[1] R.M.O. Galvão, et al., Report on recent results obtained in TCABR, J. Phys. (2015) 012001, https://doi.org/10.1088/1742-6596/591/1/012001.
[2] G. Canal, et al., An Overview of the Upgrade of the TCABR Tokamak, 2019. https://inis.iaea.org/search/search.aspx?orig_q=RN:53079978 (Accessed 25 October 2023).
[3] P. Santra, V. Bedakihale, T. Ranganath, Thermal structural analysis of SST-1 vacuum vessel and cryostat assembly using ANSYS, Fusion Eng. Des. 84 (7–11) (2009) 1708–1712, https://doi.org/10.1016/j.fusengdes.2009.01.042.
[4] S. Yuntao, et al., Static and dynamic mechanical analyses for the vacuum vessel of EAST superconducting tokamak device, Plasma Sci. Technol. 8 (2) (2006) 221, https://doi.org/10.1088/1009-0630/8/2/21.
[5] S. Cho, et al., Thermohydraulic design of the KSTAR vacuum vessel, Fusion Eng. Des. 58 (2001) 851–855, https://doi.org/10.1016/S0920-3796(01)00482-3.
[6] P.M. Anderson, A.G. Kellman, Optimized baking of the DIII-D vessel, in: 18th IEEE/NPSS Symposium on Fusion Engineering. Symposium Proceedings (Cat. No. 99CH37050), IEEE, 1999, pp. 535–538, https://doi.org/10.1109/FUSION.1999.849896.
[7] Y. Feldshteyn, et al., TPX vacuum vessel transient thermal and stress conditions, in: Proceedings of 16th International Symposium on Fusion Engineering, IEEE, 1995, pp. 1311–1314, https://doi.org/10.1109/FUSION.1995.534468.
[8] V. Tanchuk, et al., System design and engineering for baking of the KTM vacuum vessel, Fusion Eng. Des. 136 (2018) 759–765, https://doi.org/10.1016/j.fusengdes.2018.04.005.
[9] A.P. Khvostenko, et al., Prebaking of T-15MD vacuum vessel, Fusion Eng. Des. 146 (2019) 2205–2208, https://doi.org/10.1016/j.fusengdes.2019.03.153.
[10] Y. Huang, et al., Thermal mechanical characteristics research of HL-2M vacuum vessel during baking, Fusion Eng. Des. 185 (2022) 113322, https://doi.org/10.1016/j.fusengdes.2022.113322.
[11] S. Pak, et al., Numerical simulation on bake-out of the ITER diagnostic upper port plug, Fusion Eng. Des. 85 (7–9) (2010) 1627–1631, https://doi.org/10.1016/j.fusengdes.2010.04.059.
[12] ANSYS User's Manual, ANSYS Inc. PA, USA.
[13] ASME, Boiler and Pressure Vessel Code, Section VIII – Rules for Construction of Pressure Vessels, Division 2 – Alternative Rules, 2007.
[14] A.D. Cheetham, et al., The TCA Tokamak-Project Report 1979, 1980. https://infoscience.epfl.ch/record/120713 (Accessed 5 January 2024).
[15] Y.A. Cengel, Heat and Mass Transfer: A Practical Approach, 3rd ed., Mc-Graw Hill, 2009.
[16] A. Bejan, Convection Heat Transfer, 2nd ed., John Wiley & Sons, 1995.
[17] W.M. Rohsenow, et al., Handbook of Heat Transfer, 3rd ed., McGraw-Hill, New York, 1998.
[18] ASME, Boiler and PressureVessel Code, Section II – Materials, Part D – Properties (Metric), 2010.